Journal of
Pharmaceutical and BioTech Industry

MDPI

Article

PMSSO-Hydrogels as a Promising Carrier for B_{12} Vitamin

Daniil Ialama [1], Polina Orlova [1], Anna Skuredina [1], Ivan Meshkov [2], Aziz Muzafarov [2] and Irina Le-Deygen [1,*]

[1] Department of Chemical Enzymology, Faculty of Chemistry, Lomonosov MSU, 119234 Moscow, Russia; saquoq@yandex.ru (D.I.); p.orlova2021@mail.ru (P.O.); skuredinanna@gmail.com (A.S.)
[2] Enikolopov Institute of Synthetic Polymeric Materials, Russian Academy of Sciences (ISPM RAS), 117393 Moscow, Russia; aziz@ispm.ru (A.M.)
* Correspondence: i.m.deygen@gmail.com

Abstract

The development of novel dosage forms of vitamin B_{12} is an urgent task for addressing vitamin deficiency in individuals with gastrointestinal diseases or those following stringent dietary limitations. The study illustrates the fundamental possibility of employing a non-toxic and biocompatible organosilicon hydrogel with significant sorption capacity for B_{12} delivery. Research indicated that 40 min of incubation suffices for optimal loading efficiency, influenced by both external diffusion and intradiffusion factors. The release of B_{12} in a medium that mimics the human gastrointestinal tract transpires almost entirely within a timeframe that aligns with physiological conditions. Consequently, organosilicon hydrogels serve as potential vehicles for the administration of vitamin B_{12}.

Keywords: hydrogels; drug delivery system; B_{12} vitamin

check for updates

Academic Editor: Fernando Albericio

Received: 30 April 2025
Revised: 7 June 2025
Accepted: 20 June 2025
Published: 23 June 2025

Citation: Ialama, D.; Orlova, P.; Skuredina, A.; Meshkov, I.; Muzafarov, A.; Le-Deygen, I. PMSSO-Hydrogels as a Promising Carrier for B_{12} Vitamin. *J. Pharm. BioTech Ind.* **2025**, *2*, 10. https://doi.org/10.3390/jpbi2030010

Copyright: © 2025 by the authors. Licensee MDPI, Basel, Switzerland. This article is an open access article distributed under the terms and conditions of the Creative Commons Attribution (CC BY) license (https://creativecommons.org/licenses/by/4.0/).

1. Introduction

In recent years, vegetarianism and its stricter variation, veganism, have been gaining increasing popularity among the population. In some cases, such a diet may be a necessary avoidance of animal-derived products to treat diseases and/or support medical treatments [1]. Therefore, an individual's condition, including cardiovascular system parameters, is carefully monitored by physicians. They ensure the necessary balance of micro- and macro-elements, hormone levels, and vitamins. Consequently, this dietary system is designed to support and improve the individual's well-being and facilitate the treatment process.

In other cases, voluntary vegetarianism has become popular among the general population due to growing awareness of its advantages. These include animal welfare, reduced risk of infections transmitted from animals to humans (such as helminthiasis), the widespread availability of plant-based foods in many regions, high fiber content in the diet, and other health benefits. However, the main drawback of voluntarily vegetarianism is the deficiency of compounds that can only be obtained from animal-derived foods, for instance, animal proteins, specific fatty acids, several trace elements (iron, zinc, selenium), and some vitamins. As a result, the World Health Organization (WHO) recommends that vegetarians take various supplements and dietary additives to compensate for the deficiency [2].

One of the most significant issues is vitamin B_{12} deficiency among vegetarians. The daily requirement for B_{12} in adults is 2–6 µg [3]. However, B_{12} is found exclusively in animal-derived foods such as meat and fatty milk. Plant-based foods contain only trace

amounts of vitamin B_{12} [4]. As an enzyme cofactor, B_{12} plays a key role in crucial metabolic processes; thus, the B_{12} deficiency can lead to severe health problems.

On the other hand, vitamin B_{12} deficiency can result from several factors: inadequate dietary intake, lack of intrinsic factor, limited bioavailability, surgical procedures, aging, and more. The treatment includes intramuscular injection (often at intervals of 2–3 months) or oral tablet forms with a high vitamin content. Oral vitamin delivery systems represent a viable alternative to intramuscular injections [5]. To date, no adverse effects have been identified in such cases, so there is no established upper safe limit for B_{12} dosage [6,7]. However, numerous recent studies have focused on the rational use of B_{12}: the decrease of dosage by improving the vitamin's stability and bioavailability in the gastrointestinal tract. This goal can be achieved using drug delivery systems [8,9].

Therefore, vegetarians and patients from the risk groups are advised to consume supplements containing the recommended daily amount of vitamin B_{12} [10].

An effective approach to the development of non-animal-based dietary supplements involves encapsulation of precise vitamin B_{12} dosage in drug delivery systems, for example, polymers that can effectively adsorb the bioactive compound and exhibit pH-responsive release from the matrix [11,12]. Recently, we demonstrated the successful sorption of iron compounds and their complexes with cyclodextrins by silicon-organic polymethylsilsesquioxane hydrogels (PMSSO). The promising results allowed us to highlight the other perspectives of PMSSO as a drug delivery system for more complicated molecules, such as B_{12} [13,14]. Modified silicas are suitable carriers for vitamin B_{12}, as these materials are already widely applied in dietary additives, intestinal sorbents, cosmetic formulations, and pharmaceutical products [15,16]. The well-known physicochemical properties of silicas (a large specific surface area that ensures high sorption capacity; thermal stability; chemical inertness; biocompatibility) make the polymer an advantageous carrier for vitamin B_{12} [17]. Compared to polypeptide- or lipid-based B_{12} delivery systems, polymer carriers have shown prospective experimental results and offer broader possibilities for modification [8].

Here we investigate the patterns of sorption and desorption of vitamin B_{12} in PMSSO-hydrogel to uncover its potential as an effective vitamin carrier for future application to the support and/or treatment of B_{12} deficiency.

2. Materials and Methods

2.1. Materials

Sodium chloride (NaCl, 58.44 g/mol, purity 99.9%, Reakhim, Moscow, Russia), potassium phosphate monobasic (KH_2PO_4, 136.09 g/mol, purity $\geq$ 99%, Sigma Aldrich, St. Louis, MO, USA), sodium phosphate dibasic (Na_2HPO_4, 141.96 g/mol, purity $\geq$ 99%, Sigma Aldrich, St. Louis, MO, USA), Cyanocobalamin B_{12} (0.5 mg/mL, Mosagrogen, Russia), 0.9% NaCl solution (saline solution for injection, Solopharm, St. Petersburg, Russia). PMSSO-hydrogel was provided by Dr. Alexandra Kalinina (1:1 $MeSiO_{1.5}/SiO_2$ links molar ratio, specific surface area 278.7 $\pm$ 4.5 m^2/g) [14]. The structure of PMSSO-hydrogel is shown in Figure 1.

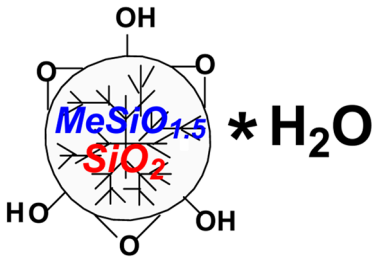


Figure 1. The structure of PMSSO-hydrogel (1:1 $MeSiO_{1.5}/SiO_2$ links molar ratio).

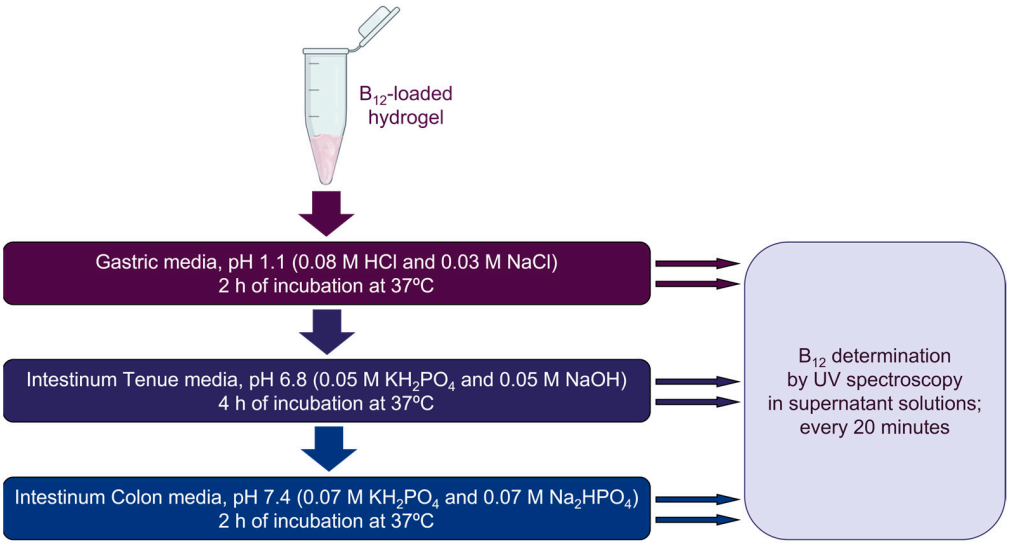
2.2. Methods

2.2.1. B_{12} Sorption into PMSSO-Hydrogel

First, 100 mg of PMSSO-hydrogel was soaked in 1 mL of a vitamin B_{12} solution (0.3 mg/mL). The system was thoroughly mixed and incubated at the temperature of 22 °C and a stirring speed of 150 rpm. Between 5 and 120 min, 20 µL of the supernatant solution was collected and diluted in 580 µL of physiological saline. Then, the UV absorption spectra of the resulting samples were recorded. Based on the obtained optical density at the maximum wavelength at 361 nm, the concentration of loaded B_{12} was calculated. After that the sorption curve was analyzed.

2.2.2. B_{12} Release

The B_{12} release was carried out in three buffer systems that imitate digestive media in order to imitate the gastro-internal tract in vitro according to the American Pharmacopeia and previously published protocols [14]. The main pipeline of the experiment is presented on Scheme 1.



Scheme 1. The pipeline of the release experiment.

Briefly, 100 mg of PMSSO-B_{12} was added to 2 mL of the gastric medium (pH 1.1), containing 0.08 M HCl and 0.03 M NaCl. After 2 h of incubation at 37 °C, the sample was transferred to the Intestinum Tenue medium (I.T.), which consisted of 0.05 M KH_2PO_4 and 0.05 M NaOH (pH 6.8), and incubated for 4 h, followed by incubation in the Intestinum Colon medium (I.C.), containing 0.07 M KH_2PO_4 and 0.07 M Na_2HPO_4 (pH 7.4), for 2 h. Every 20 min, a sample of 2 mL was collected, and a fresh portion of the medium was added to the gel. The UV absorption spectrum for the selected solutions was recorded to monitor the concentration of desorbed vitamin B_{12}.

2.2.3. Spectroscopy Studies

The UV-spectra were recorded with an Ultrospec 2100 pro instrument (Amersham Biosciences, Amersham, UK) within a wavelength range of 200–500 nm in a 1 mL quartz cell (Hellma Analytics, Müllheim, Germany).

2.2.4. Mathematical Processing of the Data

Sorption curves were studied using pseudo-first-order and pseudo-second-order kinetics, according to Equations (1) and (2).

$$A_t = A_\infty\left(1 - e^{k_1 t}\right) \quad (1)$$

$$A_t = \frac{A_\infty^2 k_2 t}{1 + A_t k_2 t} \quad (2)$$

where A_t is the amount of sorbed B_{12} at time t, A_∞ is the amount of sorbed B_{12} at equilibrium, and k_1 and k_2 are the rate constants of the sorption process.

Equations (3) and (4), representing the Boyd–Adamson model for external and internal diffusion, respectively, are as follows:

$$\ln(1 - A_t/A_\infty) = -C \times t \quad (3)$$

$$A = f\left(\sqrt{t}\right) \quad (4)$$

where C is an empirical constant.

For the studies of intradiffusion processes, the Weber–Morris model was applied with Equation (5):

$$A_t = k_{id}\sqrt{t} + c \quad (5)$$

where k_{id} is the rate constant of internal diffusion and c is a parameter related to the thickness of the boundary layer.

Drug release models were considered as follows. The zero-order release model is described using Equation (6):

$$Q_t = Q_\infty + K_0 t \quad (6)$$

where K_0 is the zero-order release constant, min^{-1}; Q_t is the amount of substance released at time t; Q_∞ is the total amount of substance released.

The first-order release model corresponds to Equation (7):

$$Q_t = Q_\infty \times e^{-K_1 t} \quad (7)$$

where K_1 is the first-order release constant, min^{-1}.

The Korsmeyer–Peppas release is described using the ratio (8):

$$\frac{Q_t}{Q_\infty} = K \times t^n \quad (8)$$

where n is the release index; K is the degree of release constant, min^{-1}.

The Higuchi release model is represented by a complex relationship (9):

$$Q_t = A \times \sqrt{\frac{D \times \varepsilon}{\tau} \times (2 \times C - \varepsilon \times C_s) \times C_s \times t} = K_H \times \sqrt{t} \quad (9)$$

where K_H is the Higuchi dissolution constant, $min^{-1/2}$; A is the unit of surface from which the amount of substance Q_t during time t; D is the diffusion coefficient, sm^2/min; C is the initial concentration of the released substance; C_s is the solubility of the substance in the matrix; ε is the porosity of the matrix (the number of channels and pores); τ is the tortuosity factor of the capillary system of the matrix (the value of the radius and branching of the channels and pores of the matrix).

2.2.5. Statistical Analysis

All experiments were triplicated, and the results were expressed as the mean value ± standard deviation, SD (n = 3). AtteStat 3.04 for Microsoft Excel was used for statistical analysis. Significance was analyzed using the Mann–Whitney test, with $p \leq 0.05$ considered statistically significant.

3. Results and Discussion

3.1. B_{12} Vitamin Sorption—Role of the Temperature

To investigate the vitamin B_{12} sorption process in PMSSO-hydrogels, we applied UV-VIS spectroscopy, as vitamin B_{12} exhibits a pronounced absorption band at 361 nm. Figure 2 illustrates the structure of vitamin B_{12} and the calibration curve (saline solution), which exhibits linearity throughout a broad concentration range. The sensitivity coefficient is $(29.2 \pm 0.3) \times 10^3$ L/(mol × cm), signifying the method's great sensitivity to the concentration of vitamin B_{12} in the solution. The detection limit is 2.0 ± 1.0 µg/mL. The determined extinction coefficient $\varepsilon = (29.2 \pm 0.3) \times 10^3$ L/(mol × cm) aligns well with the literature values [18].

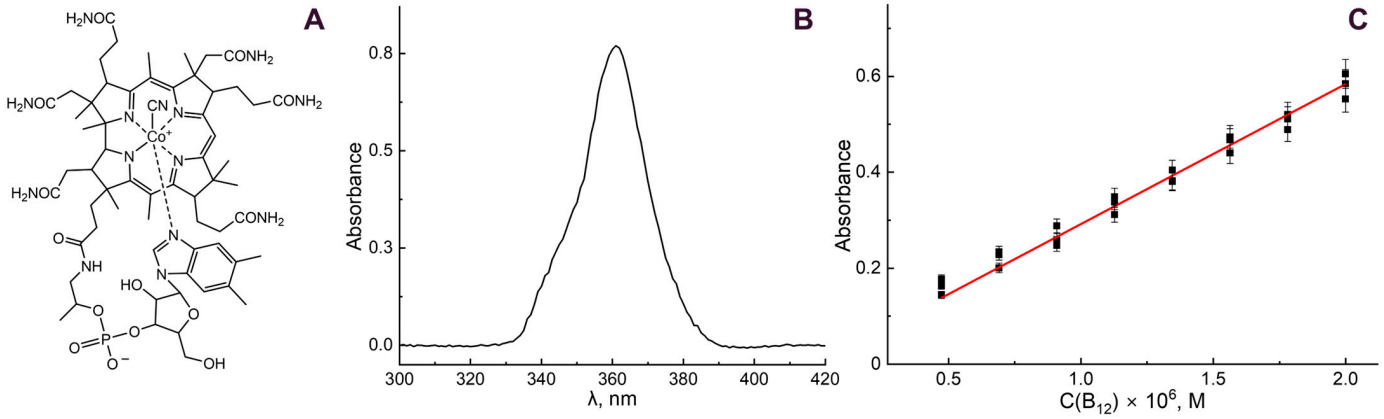


Figure 2. (**A**) B_{12} structure, (**B**) B_{12} UV-VIS band at 361 nm, and (**C**) B_{12} calibration curve for the UV-VIS band (λ = 361 nm, 0.9% NaCl solution, 22 °C).

The incubation temperature can significantly affect the sorption processes of active compounds in gels. We investigated the kinetic of sorption equilibrium by incubating PMSSO-hydrogels in a vitamin B_{12} solution for 120 min at 22 °C (Figure 3).

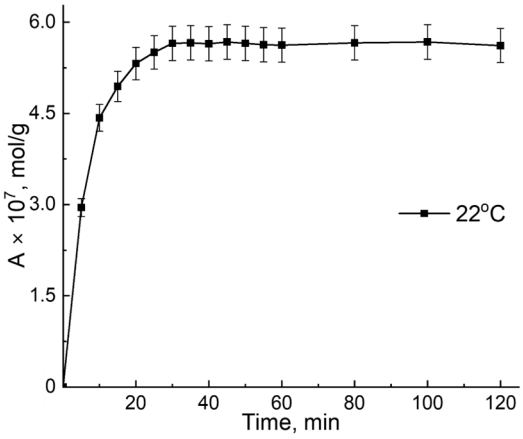


Figure 3. Integral kinetic PMSSO-B_{12} sorption curves (0.9% NaCl solution, 22 °C).

The analysis of the curve indicates that sorption equilibrium is attained promptly, after ≈40 min. The concentration of B_{12} after sorption calculated using the UV-VIS calibration curve was 1.65×10^{-4} M, whereas the concentration of the initial solution was $\frac{0.3}{1355.38} \approx 2.22 \times 10^{-4}$ M. The amount of sorbed B_{12} per 100 mg of the carrier was $(2.22 - 1.65) \times 10^{-4} \times 1000 \times 1355.38 \approx 77\ \mu g$.

Thus, the degree of B_{12} extraction from the solution was 25.7% (10):

$$\alpha = \frac{77}{0.3 \times 1 \times 1000} \times 100\% \approx 25.7\% \quad (10)$$

The sorption capacity of the PMSSO-hydrogel can be calculated as the mass or amount of B_{12} sorbed per 1 g of sorbent:

$$A = \frac{77}{0.1000 \times 1000} \approx 0.77\ mg/g \quad (11)$$

$$A = \frac{77 \times 10^{-6}}{1355.38 \times 0.1000} \approx 5.7 \times 10^{-7}\ mol/g \quad (12)$$

Compared to the previously published data, the highest sorption capacity of the carrier for B_{12} in the literature is characteristic of inorganic materials. For example, loading B_{12} into nanolayers of montmorillonite yields 20–160 mg per 1 g of sorbent [19], while mesoporous carbon particles have achieved a record 486 mg of B_{12} per 1 g of the delivery system [20]. For organic polymer carriers, apparently due to high hydrophilicity, the sorption capacity of the carriers is significantly lower. Thus, the highest value (15–25 mg/g) was found when encapsulating B_{12} in crosslinked carboxymethyl pullulan [21]. However, other studies mention values close to our data, for example, 1% by weight for poly(acrylic acid) microspheres (modified or unmodified with cysteine) [22], or 0.21 mg/g for soy protein nanoparticles [23].

The initial increase in sorption, followed by a plateau as equilibrium is reached, may suggest that at the beginning of experiment, B_{12} molecules transfer from the solution to the active sites of the gel and then bind to the sorbent's surface (apparently to the –OH groups). The sorption curve may be divided into two segments: the initial rising region and the plateau. The mathematical analysis of both regions may provide detailed insight into the interaction mechanism between B_{12} molecules and PMSSO [24].

3.2. B_{12} Vitamin Sorption: Looking for the Mathematical Model

The kinetics of B_{12} sorption into PMSSO were approximated using first- and second-order models, as shown in Equations (1) and (2), and the corresponding kinetic parameters are summarized in Table 1.

Table 1. Rate constants of the first- and second-order of sorption kinetics (p = 0.95, n = 3).

α, %	A_t, mg/g	Pseudo-First Order			Pseudo-Second Order		
25.7	0.77	A_t, mg/g 0.766 ± 0.01	k_1, min^{-1} 0.147 ± 0.008	R^2 0.99	A_t, mg/g 0.83 ± 0.06	k_1, g/(mg × min) 0.303 ± 0.012	R^2 0.98

Figure 4 shows the linear anamorphosis of the experimental kinetic data describing the pseudo-first and pseudo-second order. The pseudo-second-order kinetic equations describe experimental data over the entire time interval, while the pseudo-first-order model describes only the initial stages of the process. This can be considered as a sign of nonlinear sorption of active molecules when filling the main binding sites.

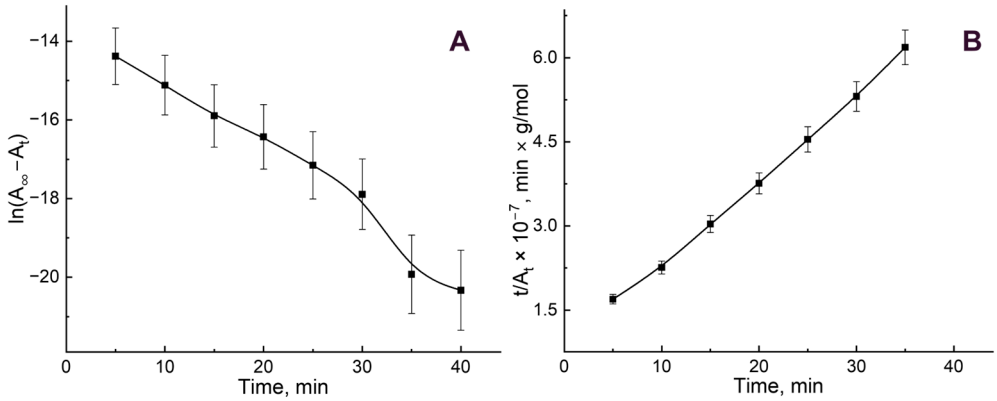


Figure 4. Anamorphosis of the kinetic sorption curve of the B_{12} molecule on the PMSSO-hydrogel in the coordinates of the model equations of the pseudo-first (**A**) and pseudo-second order (**B**).

In order to study this process in detail, the sorption of B_{12} molecules from the solution to the bulk phase of the PMSSO was analyzed using the Boyd–Adamson model for external and internal diffusion and the Weber–Morris model for internal diffusion [25]. The Boyd–Adamson model was applied using Equations (3) and (4), which describe external and internal diffusion, respectively. This approach has proven itself in a number of studies, for example, in the analysis of the sorption of copper compounds into the matrix of the natural polysaccharide chitosan [26].

The obtained data are shown in Figure 5A,B. Comparing these graphs, one could conclude that neither external nor internal diffusion are unambiguously limiting the sorption process, which may be due to the uneven distribution of the PMSSO pore size. At the initial stages of sorption, the limiting process is probably external diffusion (external diffusion mass transfer), and at the final stages, when most of binding sites are already loaded of sorption, internal.

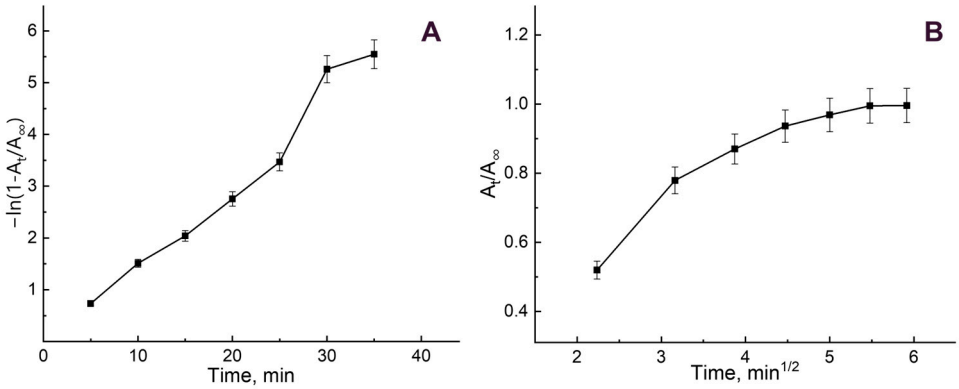


Figure 5. The external (**A**) and internal (**B**) diffusion of cyanocobalamin molecules, represented in the coordinates of the Boyd–Adamson model for PMSSO-hydrogel.

For the further studies of intradiffusion processes, we have applied the Weber–Morris model according to Equation (5). The obtained data are shown in Figure 6.

The curve in the coordinates of the Weber–Morris model (Figure 6) is not linear, indicating the sorption process is not uniquely limited by external and internal diffusion, which agrees with the conclusions drawn from the Boyd–Adamson theory, similar to the previously published paper [26]. The multilinearity of the dependence of the Weber–Morris model indicates a multi-stage interaction of sorbate and sorbent.

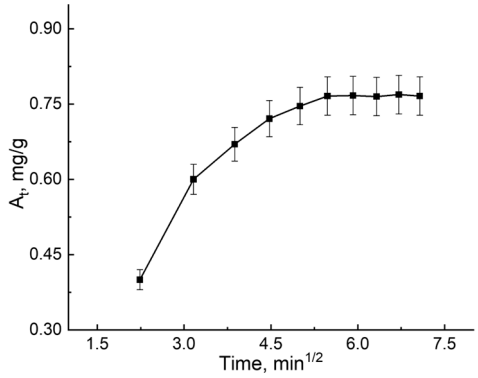


Figure 6. The process of internal diffusion of B_{12} molecules into PMSSO-hydrogel according to the Weber–Morris model.

In the sorption process (Figure 3), three successive stages of mass transfer of cyanocobalamin can be distinguished. The first linear section characterizes the diffusion of B_{12} from the volume of the solution through the outer diffusion layer to the PMSSO surface, which is limited by the stage of diffusion through the boundary at the surface. After the breaking point, the role of external diffusion processes decreases, and the role of intra-diffusion processes rises. The second linear region corresponds to the diffusion of B_{12} into PMSSO-hydrogel through a layer of already sorbed molecules deep into the gel through the systems of pores and capillaries. The intradiffusion process is limited by the transfer of molecules in the sorbent phase. The third and final linear region corresponds to the interaction of B_{12} with the binding sites of the PMSSO-hydrogel: the B_{12} molecule has a cyano group and a cobalt center, which can react with hydroxy groups on the sorbent surface by forming coordination bonds. At this point, an equilibrium of B_{12} concentration has been established between the solid and liquid phases [27]. Hydroxyl groups can form hydrogen bonds with hydrogen or oxygen atoms in the B_{12} molecule, providing a strong binding of the molecule to the surface of the sorbent.

Similar results were recently obtained for crystal violet and eosin sorption in the organic carries [28]. The results of mathematical processing using the Weber–Morris model for each site are presented in Table 2.

Table 2. Internal diffusion parameters according to the Weber–Morris model (p = 0.95, n = 3).

Step	k_{id}, mg/(g × $min^{1/2}$)	c, mg/g	R^2
1	0.216	0.08	1
2	0.059 ± 0.008	0.45 ± 0.04	0.96
3	0.045 ± 0.002	0.52 ± 0.01	0.99

To assess the influence of the chemical stage on the sorption process in a solid-liquid phase system, it is convenient to use pseudo-first and pseudo-second-order models in linear form [29]. The results of processing according to these models are shown in Figure 3. According to the obtained data, the pseudo-first-order kinetic equation describes experimental data at the initial and intermediate stages of the process, and the pseudo-second-order model refers to the entire time interval. The coefficients for each model are 0.967 and 0.998, respectively. The correspondence of the experimental sorption data to the pseudo-second-order kinetic equation indicates that the interaction between B_{12} molecules and the binding sites of the sorbent follows pseudo-second-order kinetics, where the rate of interaction is proportional to the product of the concentrations of the two reactants.

Discussing the obtained data, we would like to put forward a hypothesis about the possible mechanism of B_{12} sorption in PMSSO-hydrogel. PMSSO-hydrogels are well-known

organo-silicon carriers for various types of compounds [30]. Initial PMSSO-hydrogels do not contain special binding cites and the main mechanism of sorption could be considered as non-specific [13]. However, after certain modifications, one could achieve higher sorption effectiveness, as we have demonstrated recently in [31]. Here we consider initial non-modified PMSSO-hydrogel as a biocompatible and safe carrier, while for modified hydrogels one must prove it before even preclinical studies. As a potential binding site, we could consider hydroxyl groups of PMSSO capable to bind with carboxyl groups and amides in B_{12} structure. Thus, according to our data, the sorption of B_{12} could be described as a combination of two processes: non-specific sorption via weak interactions and sorption supported by hydrogen bonds formation. This combination provides considerable values of loading efficacy.

Thus, mathematical processing of the integral kinetic curve of B_{12} sorption into the PMSSO-hydrogel showed that during the sorption process, the combined effect of diffusion and chemical reaction is observed, and the sorption occurs in a diffusion mode.

3.3. B_{12} Vitamin Release from PMSSO-Hydrogel in the Digestive Medium

The release curve of B_{12} from PMSSO-hydrogel in buffer solutions imitating the gastric, small, and large intestines is demonstrated in Figure 7.

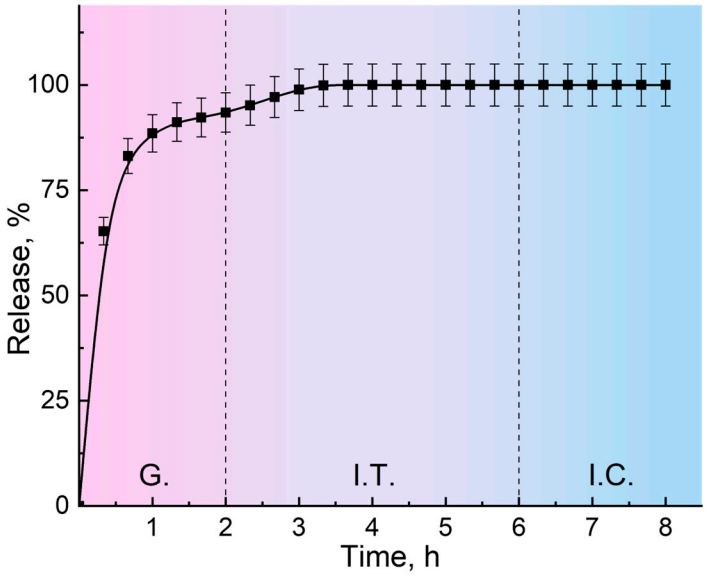


Figure 7. The release curve of B_{12} from PMSSO-hydrogel (G.—Gastric medium: 0.08 M HCl and 0.03 M NaCl, pH 1.1, 37 °C, 2 h; I.T.—Intestinum Tenue medium: 0.05 M KH_2PO_4 and 0.05 M NaOH, pH 6.8, 37 °C, 4 h; I.C.—Intestinum Colon medium: 0.07 M KH_2PO_4 and 0.07 M Na_2HPO_4, pH 7.4, 2 h).

Firstly, there is a rapid release of the vitamin in the gastric medium till 90% of loaded into PMSSO. The remaining 10% release at the slightly alkaline environment of the small intestine. According to Figure 7, about 69 μg B_{12} is released in an acidic environment and 7.6 μg in a slightly alkaline environment. This behavior of the release curve can be explained by the H^+ interaction with the hydroxyl groups of the PMSSO-hydrogel displacing the B_{12} associated with gel. In a slightly alkaline environment, the stability of the PMSSO-hydrogel decreases—hydroxyl groups from the solution contribute to the gradual destruction of the siloxane skeleton of the hydrogel and its dissociation. As a result, we observed the complete dissolution of PMSSO. From the point of view of vitamin B_{12} delivery, the result is an advantage, since the degradation of the hydrogel produces safe products, and the drug is completely released.

Many factors, such as the type of dosage form and its solubility, the crystallinity of the matrix, the size of the particles, the acidity of the medium, etc., influence the release behavior [16]. Therefore, mathematical models are used to study the kinetics and establish the mechanism of drug release from drug delivery systems [32].

For the delivery systems based on solid-liquid phase systems, where polymer carriers act as a matrix, it is most convenient to use zero- and first-order models, as well as the Higuchi and Korsmeyer–Peppas models. The zero-order release model is used to describe osmotic systems, low-soluble release matrix systems, transdermal systems, and drug-coated systems. In this model there is a linear relationship between the degree of drug dissolution and time, and release is a diffusion process. The first-order release model reflects the process of dissolution of solid particles in a liquid medium and characterizes the release process as a diffusion process according to Fick's first law, which governs most polymer carrier delivery systems [33].

The Korsmeyer–Peppas release model is a semi-empirical model based on diffusion mechanisms in polymeric systems [34]. In case diffusion is the primary mechanism of drug release, the graph of the amount of substance released from the square root of time is represented by a straight line, and if the mechanism of release is different from Fick's law, then a straight-line relationship will be observed depending on the equation above.

The Higuchi model describes a diffusion release that obeys Fick's first law and is linearly dependent on the square root of time. To use the Higuchi model, several conditions must be met: the swelling and dissolution of the matrix are limited or insignificant, the initial concentration of the released substance in the matrix exceeds its solubility, and the size of the system is much larger than the size of the particles (molecules) released from it [33]. Among other things, the immersion condition must always be achieved in the environment.

The B_{12} molecule release curve can be divided into three parts: two ascending sections, one of which is steeper and faster (in an acidic medium), and the other, more uniform and straight, has a smaller slope (slightly alkaline medium), and the remaining part of the profile is a plateau. The upward sections of the release profile were processed according to the above mathematical models of release kinetics. The results of mathematical processing for each of the two ascending sections of the curve are shown in Table 3. The differences between some R^2 values are insignificant, which necessitates further consideration of the features of the organosilicon matrix of the hydrogel and the physical laws governing release kinetics, as typically described using the Higuchi and Korsmeyer–Peppas models.

Table 3. B_{12} release constants from PMSSO-hydrogel for different models of release kinetics (p = 0.95, n = 3).

Q_∞, μg	Step	Zero-Order Release Model			Korsmeyer-Peppas Release Model		
		Q_∞, μg	K_0, min^{-1}	R^2	K, min^{-1}	n	R^2
76.6	1	53.3 ± 3.6	0.318 ± 0.096	0.85	32.1 ± 0.3	0.25 ± 0.04	0.98
	2	70.6 ± 0.2	0.062 ± 0.003	0.992	52.6 ± 0.1	0.12 ± 0.01	0.99
		First-Order Release Model			Higuchi Release Model		
		Q_∞, μg	K_1, min^{-1}	R^2	K_H, $min^{-1/2}$		R^2
	1	69.8 ± 0.4	0.062 ± 0.002	0.998	5.78 ± 1.28		0.98
	2	76.3 ± 0.7	0.025 ± 0.002	0.88	1.95 ± 0.09		0.99

Thus, the Higuchi and Korsmeyer–Peppas models (n < 0.5) allow us to consider the process of release of cyanocobalamin molecules from PMSSO-hydrogel as a diffusion process obeying Fick's first law in an acidic and slightly alkaline environment. The release exhibits delayed kinetics at the final stages in a slightly alkaline environment and rapid

kinetics in an acidic medium, which follows from the obtained values of the release and dissolution constants. Considering hydrogen bond formation and non-specific sorption as the main forces supporting B_{12} loading onto the hydrogel, acidic medium could indeed lead to enhanced release.

The key processes of vitamin B_{12} metabolism in the human body occur in the stomach, namely, the binding of cyanocobalamin molecules to the Castle factor for their subsequent absorption into the blood in the upper small intestine via receptor-mediated endocytosis [35]. Comparing the release curve with the mechanism of metabolism indicates that the cyanocobalamin delivery system based on PMSSO-hydrogel is effective, since most of the vitamin is released in the stomach.

4. Conclusions

This study examined the feasibility of using PMSSO-hydrogel as a B_{12} carrier to support and/or treat the vitamins deficiency. UV-VIS spectroscopy served as a main analytical technique for quantifying the vitamin's content. This method exhibits appropriate sensitivity and precision for low concentrations. The detection limit of cyanocobalamin in its solutions is 2 ± 1 μg/mL. The measurable concentration range was from 6 ± 1 μg/mL to 56 ± 3 μg/mL.

We successfully optimized the conditions for the sorption of cyanocobalamin in PMSSO-hydrogel by determining the process temperature and the contact duration of the polymer matrix with the B_{12} solution at 37 °C. The hydrogel exhibits mixed-diffusion mode sorption of B_{12}. The examination of the cyanocobalamin release profile from the PMSSO-hydrogel in a system mimicking the human gastrointestinal tract indicated that the release transpires through a diffusion process adhering to Fick's first law and is optimally characterized using the Korsmeyer–Peppas and Higuchi models. A fast release of the active molecule occurs in an acidic medium, linked to the protonation of the hydrogel's active sites. In a mildly alkaline environment, the process progressively decelerates and becomes linear, while the hydrogel eventually disintegrates due to the dissociation resulting from the degradation of the siloxane framework.

The developed system could be considered as a perspective vitamin B_{12} delivery system with a prolonged release profile.

Author Contributions: Conceptualization, A.S., I.M., A.M. and I.L.-D.; Data curation, D.I. and P.O.; Formal analysis, D.I. and P.O.; Investigation, D.I. and P.O.; Methodology, P.O., I.M., A.M. and I.L.-D.; Project administration, I.L.-D.; Supervision, I.L.-D.; Visualization, D.I.; Writing—original draft, P.O. and I.L.-D.; Writing—review & editing, D.I. and A.S. All authors have read and agreed to the published version of the manuscript.

Funding: This study is supported with the program Students startups No. 4509ГССС15-L/102591 by Foundation for assistance to small innovative enterprises (Author P.O.). Synthesis of the sorbents were carried out with the financial support from Ministry of Science and Higher Education of the Russian Federation using the equipment of Collaborative Access Center "Center for Polymer Research" of ISPM RAS (FFSM-2024-0001).

Data Availability Statement: All original raw data are available upon request from the authors.

Conflicts of Interest: The authors declare no conflicts of interest.

Abbreviations

WHO	World Health Organization
PMSSO-hydrogel	Polymethylsilsesquioxane hydrogel
G	Gastric medium
IT	Intestinum Tenue medium

IC	Intestinum Colon medium

References

1. Emelyanova, A.Y.; Zinovyeva, O.E. Vitamin B_{12} in the Treatment of Nervous System Diseases. *RMJ* **2016**, *24*, 429–433.
2. WHO European Office for the Prevention and Control of Noncommunicable Diseases. *Plant-Based Diets and Their Impact on Health, Sustainability and the Environment: A Review of the Evidence*; WHO Regional Office for Europe: Copenhagen, Denmark, 2021.
3. Doets, E.L.; Veld, P.H.; Szczecińska, A.; Dhonukshe-Rutten, R.A.M.; Cavelaars, A.E.J.M.; van't Veer, P.; Brzozowska, A.; de Groot, L.C.P.G.M. Systematic Review on Daily Vitamin B_{12} Losses and Bioavailability for Deriving Recommendations on Vitamin B_{12} Intake with the Factorial Approach. *Ann. Nutr. Metab.* **2013**, *62*, 311–322. [CrossRef] [PubMed]
4. Hannibal, L.; Lederer, A.K.; Storz, M.A.; Huber, R.; Jacobsen, D.W. Vitamin B_{12} Status and Supplementation in Plant-Based Diets. *Food Nutr. Bull.* **2024**, *45* (Suppl. S1), 58–66. [CrossRef]
5. Abdelwahab, O.A.; Abdelaziz, A.; Diab, S.; Khazragy, A.; Elboraay, T.; Fayad, T.; Diab, R.A.; Negida, A. Efficacy of different routes of vitamin B_{12} supplementation for the treatment of patients with vitamin B_{12} deficiency: A systematic review and network meta-analysis. *Ir. J. Med. Sci.* **2024**, *193*, 1621–1639. [CrossRef]
6. Green, R.; Allen, L.H.; Bjørke-Monsen, A.L.; Brito, A.; Guéant, J.L.; Miller, J.W.; Molloy, A.M.; Nexo, E.; Stabler, S.; Toh, B.H.; et al. Vitamin B_{12} deficiency. *Nat. Rev. Dis. Primers* **2017**, *3*, 17040. [PubMed]
7. Green, R.; Miller, J.W. Vitamin B_{12} Deficiency. In *Vitamins and Hormones*; Elsevier: Amsterdam, The Netherlands, 2022; Volume 119, pp. 405–439.
8. Skuredina, A.A.; Ialama, D.E.; Le-Deygen, I.M. Vitamin B_{12} in Drug Delivery Systems (A Review). *Russ. J. Bioorg. Chem.* **2024**, *50*, 2540–2557. [CrossRef]
9. Gong, Y.; Zhang, Q.; Yuan, H.; Luo, X. Fabrication of carboxylated cellulose microspheres via Fe^{2+}/H_2O_2 oxidation method and their application in vitamin B_{12} efficient loading and controlled release. *J. Drug Deliv. Sci. Technol.* **2025**, *104*, 106515. [CrossRef]
10. Fernandes, S.; Oliveira, L.; Pereira, A.; Costa, M.D.C.; Raposo, A.; Saraiva, A.; Magalhães, B. Exploring Vitamin B_{12} Supplementation in the Vegan Population: A Scoping Review of the Evidence. *Nutrients* **2024**, *16*, 1442. [CrossRef]
11. Lopes, F.; dos Reis, A.C.; Paludo, K.S.; Tenório-Neto, E.T.; Lima-Tenório, M.K.; Viana, A.G. Designing biocompatible xanthan gum hydrogels for pH-responsive vitamin B_{12} delivery. *Int. J. Biol. Macromol.* **2025**, *308*, 142449. [CrossRef]
12. Ueoka, H.; Shimomura, O.; Ueda, K.; Inada, K.; Nomura, R. Release behavior of a polyanion-crosslinked chitosan-poly(N-isopropylacrylamide) gel thermoresponsive material. *J. Appl. Polym. Sci.* **2018**, *135*, 46732. [CrossRef]
13. Orlova, P.; Meshkov, I.B.; Latipov, E.V.; Vasiliev, S.G.; Kalinina, A.A.; Muzafarov, A.M.; Le-Deygen, I.M. Functional Design of Peroral Iron Compound Delivery Systems Based on Polymethylsilsesquioxane Hydrogels for the Therapy of Iron Deficiency Anemia. *Russ. J. Inorg. Chem.* **2024**, *69*, 428–438. [CrossRef]
14. Orlova, P.; Meshkov, I.; Latipov, E.; Vasiliev, S.; Mikheev, I.; Ratova, D.-M.; Kalinina, A.; Muzafarov, A.; Le-Deygen, I. Cyclodextrin—Polymethylsilsesquioxane Combined System as a Perspective Iron Delivery System for Oral Administration. *Gels* **2024**, *10*, 564. [CrossRef] [PubMed]
15. Kulikova, G.A.; Parfenyuk, E.V. Surface Properties of Modified Nanoscale Silicas and Their Influence on Human Serum Albumin Immobilization. *Phys. Chem. Surf. Mater. Prot.* **2010**, *46*, 473–477.
16. Gupta, A.; Bhasarkar, J.; Chandan, M.R.; Shaik, A.H.; Kiran, B.; Bal, D.K. Diffusion Kinetics of Vitamin B_{12} from Alginate and Poly(vinyl acetate) Based Gel Scaffolds for Targeted Drug Delivery. *J. Macromol. Sci. Part B* **2020**, *59*, 713–730. [CrossRef]
17. Larrañeta, E.; Domínguez-Robles, J.; Coogan, M.; Heaney, E.; Stewart, S.A.; Thakur, R.R.S.; Donnelly, R.F. Poly(methyl vinyl ether-co-maleic acid) Hydrogels Containing Cyclodextrins and Tween 85 for Potential Application as Hydrophobic Drug Delivery Systems. *Macromol. Res.* **2019**, *27*, 396–403. [CrossRef]
18. Al-Samarrai, M.Q.; Al-Samarrai, K.F. Determination of Riboflavin and Cyanocobalamine Spectrophotometricaly via Area Un-der Curve Method. *Tikrit J. Pure Sci.* **2023**, *22*, 139–145. [CrossRef]
19. Afarani, Z.R.; Sarvi, M.N.; Alavijeh, M.A. Modification of montmorillonite nanolayers as a pH-responsive carrier of biomolecules: Delivery of vitamin B_{12}. *J. Taiwan Inst. Chem. Eng.* **2018**, *84*, 19–27. [CrossRef]
20. Xu, D.P.; Yoon, S.-H.; Mochida, I.; Qiao, W.M.; Wang, Y.G.; Ling, L.C. Synthesis of mesoporous carbon and its adsorption property to biomolecules. *Microporous Mesoporous Mater.* **2008**, *115*, 461–468. [CrossRef]
21. Mocanu, G.; Nichifor, M.; Picton, L.; About-Jaudet, E.; Le Cerf, D. Preparation and characterization of anionic pullulan thermoassociative nanoparticles for drug delivery. *Carbohydr. Polym.* **2014**, *111*, 892–900. [CrossRef]
22. Sarti, F.; Iqbal, J.; Müller, C.; Shahnaz, G.; Rahmat, D.; Bernkop-Schnürch, A. Poly(acrylic acid)-cysteine for oral vitamin B_{12} delivery. *Anal. Biochem.* **2012**, *420*, 13–19. [CrossRef]
23. Zhang, J.; Field, C.J.; Vine, D.; Chen, L. Intestinal uptake and transport of vitamin B_{12}-loaded soy protein nanoparticles. *Pharm. Res.* **2015**, *32*, 1288–1303. [CrossRef] [PubMed]
24. Díaz-Marín, C.; Zhang, L.; Lu, Z.; Alshrah, M.; Grossman, J.; Wang, E. Kinetics of Sorption in Hygroscopic Hydrogels. *Nano Lett.* **2022**, *22*, 1100–1107. [CrossRef]

25. Gorshkova, R.M.; Slobodova, D.A.; Gladyshev, P.P. Diffusion Kinetics of Sorption Processes on Sorbents Based on Pectinic Polysaccharides. *Fibre Chem.* **2024**, *55*, 341–348. [CrossRef]
26. Fufaeva, V.A.; Nikiforova, T.E. Extraction of Copper Ions by Chitosan-Based Sorbents Modified with Nickel 2-Ethylimidazolate. *Prot. Met. Phys. Chem. Surf.* **2022**, *58*, 262–268. [CrossRef]
27. Hernandez-Montelongo, R.; Salazar-Araya, J.; Hernandez-Montelongo, J.; Garcia-Sandoval, J.P. Mathematical Modeling of Recursive Drug Delivery with Diffusion, Equilibrium, and Convection Coupling. *Mathematics* **2022**, *10*, 2171. [CrossRef]
28. Mehmood, A.; Bano, S.; Fahim, A.; Parveen, R.; Khurshid, S. Efficient removal of crystal violet eosin B from aqueous solution using *Syzygium cumini* leaves: Acomparative study of acidic basic dyes on a single adsorbent. *Korean J. Chem. Eng.* **2015**, *32*, 882–895. [CrossRef]
29. Rizwan, K.; Babar, Z.B.; Munir, S.; Arshad, A.; Rauf, A. Recent advancements in engineered biopolymeric-nanohybrids: A greener approach for adsorptive-remediation of noxious metals from aqueous matrices. *Environ. Res.* **2022**, *215 Pt 3*, 114398. [CrossRef] [PubMed]
30. Meshkov, I.B.; Mazhorova, N.G.; Bakirov, A.V.; Vasil'ev, S.G.; Kalinina, A.A.; Bystrova, A.V.; Muzafarov, A.M. Evolution of Methylsilsesquioxane: From Hydrolytic Polycondensation Product to Xerogel. *Polymers* **2025**, *17*, 279. [CrossRef]
31. Orlova, P.; Meshkov, I.; Sharikov, S.; Frolov, V.; Skuredina, A.; Markov, P.; Bobyleva, Z.; Lakienko, G.; Latipov, E.; Kolmogorov, I.; et al. Amidated and Aminated PMSSO-Hydrogels as a Promising Enzyme-Sensitive Vehicle for Antianemic Drugs. *Gels* **2025**, *11*, 118. [CrossRef]
32. Filippova, N.I.; Teslev, A.A. Application of Mathematical Modeling in the Evaluation of in vitro Drug Release. *Drug Dev. Regist.* **2017**, *4*, 218–226.
33. Bhasarkar, J.; Bal, D. Kinetic investigation of a controlled drug delivery system based on alginate scaffold with embedded voids. *J. Appl. Biomater. Funct. Mater.* **2019**, *17*, 2280800018817462. [CrossRef] [PubMed]
34. Pourtalebi Jahromi, L.; Ghazali, M.; Ashrafi, H.; Azadi, A. A comparison of models for the analysis of the kinetics of drug release from PLGA-based nanoparticles. *Heliyon* **2020**, *6*, e03451. [CrossRef] [PubMed]
35. Guéant, J.L.; Guéant-Rodriguez, R.M.; Alpers, D.H. Vitamin B_{12} Absorption and Malabsorption. In *Vitamins and Hormones*; Elsevier: Amsterdam, The Netherlands, 2022; Volume 119, pp. 241–274.

Disclaimer/Publisher's Note: The statements, opinions and data contained in all publications are solely those of the individual author(s) and contributor(s) and not of MDPI and/or the editor(s). MDPI and/or the editor(s) disclaim responsibility for any injury to people or property resulting from any ideas, methods, instructions or products referred to in the content.